2009 American Control Conference
Hyatt Regency Riverfront, St. Louis, MO, USA
June 10-12, 2009

Vehicle Handling Assistant Control System via Independent Rear Axle Torque Biasing

Hai Yu, Wei Liang, Ming Kuang and Ryan McGee

Abstract— **In this paper, a vehicle handling assistant control system has been developed to improve vehicle steerability and stability in dynamic vehicle handling maneuvers by utilizing electrical drivetrain based vehicle dynamic control technology. The proposed Independent axle Torque Biasing (ITB) technology takes advantage of the direct yaw control moment obtained from differential left-to-right wheel torques to achieve additional torque steering. The highly integrated control system is expected to provide more powerful and smooth vehicle dynamic control performance in a wider range of application scenarios with minimal driving interventions. The proposed ITB control system has been designed to assist the vehicle handling to be close to a linear vehicle handling characteristic in normal driving situations and to restrain the vehicle lateral dynamics to be within the stable handling region in extreme maneuvers. Simulation results are provided to demonstrate the validity and effectiveness of the proposed ITB technology in vehicle dynamic handling assistance.**

I. Introduction

Vehicle handling assistant systems and stability control systems have been extensively and intensively investigated in the automotive industry in recent years both for safety control and for handling enhancement. Different control technologies have been proposed and implemented to assist the driver in achieving a higher level of vehicle steerability and in retaining stability (no fishtailing or plowing) as well as to improve driving comfort. For steerability enhancement, active front steering (AFS) systems have been extensively studied by both the auto industry and research institutes [1][2][3]. AFS improves the vehicle steering response and helps the driver to avoid getting into critical handling situations. As the vehicle dynamics approach the handling limit and the lateral tire forces saturate, AFS becomes less effective. In order to maintain vehicle stability under critical driving conditions, the drivetrain based (e.g. torque vectoring) and the brake based (e.g. ESP) vehicle dynamic stability control (VDC) systems that utilize differential driving/braking forces between the left and right sides of the vehicle to produce the required corrective yaw moment have been developed [4][5][6][7][8]. These systems are quite powerful when the handling limit is approached because the additional yaw control moment is obtained from the biased tire longitudinal force even in the vicinity of the friction limit. Nevertheless, these control systems are either not available all the time or not desirable in normal driving situations because of the direct interference of the control action on the longitudinal vehicle dynamics and hence disturbances to the driver. A torque vectoring system may not bring unexpected vehicle motion, but its effectiveness is limited by the availability of the traction torques.

Due to the limitations of existing vehicle dynamic control technologies, it is highly desirable to have an active vehicle dynamic control system that is capable of assisting the vehicle handing and stability improvement in a wider range of vehicle handling scenarios while minimizing undesired driving interventions. Electrical vehicle propulsion is viewed as the next generation of vehicle powertrain technology. An extension to the regular hybrid electrical drivetrain structure is the in-wheel-motor electric drive system [9]. Such a distributed propulsion device provides independent wheel control in both acceleration and braking. The direct drive feature allows for differential torque biasing at a driven axle, with the option of braking with one wheel while accelerating with the other. This torque distribution capability is named as Independent axle Torque Biasing (ITB) technology. As a result, the independent driven wheels provides another steering control input, i.e. torque steering. An additional yaw moment can be generated for vehicle steering enhancement and stability improvement purposes by regulating the vehicle yaw rate and side slip motions. It is more effective in enhancing vehicle stability because the yaw moment resulting from the difference in longitudinal tire forces of the left and right wheels is less significantly influenced by lateral vehicle acceleration.

This paper will focus on applying ITB technology at the rear driven axle. As shown in Figure 1, given the total traction torque to the rear axle T_{dr}, a yaw control moment M_c can be generated by differentially distributing the drive torque between the two rear wheels:

$$T_{dr} = (F_{x3} + F_{x4})R_w \quad (1)$$

$$M_c = (F_{x3} - F_{x4})T/2 \quad (2)$$

where R_w is the effective wheel radius and T is the trackwidth. The wheel longitudinal force F_{x3} and F_{x4} have the freedom to take either a positive value or a negative value irrespective of T_{dr}. This distinguishes ITB from a common torque vectoring technology in which both F_{x3} and F_{x4} must have the same sign as that of T_{dr}. Let F_{rm} be absolute value of the maximum available rear tire force constrained by the subsystem limits, regenerative capability and the friction conditions. The total available range of the active yaw moment control torque is:

$$-F_{rm}T \leq M_c \leq F_{rm}T \quad (3)$$

The theoretical maximum of ITB yaw control moment for torque steering doubles and the ITB yaw control moment is available all the time. A wider range of application is

978-1-4244-4524-0/09/$25.00 ©2009 AACC

expected, which enables ITB to be a more valuable and promising vehicle dynamic control technology. The extended yaw control moment is obtained by offsetting the tire longitudinal forces without any compliance to the vehicle traction condition in most driving scenarios. Minimal driver's perception to the active control actions can be achieved and the resultant vehicle is more convenient to handle and more comfortable to drive. Most importantly, the proposed ITB control technology aims to constrain vehicle instability tendency before it happens.

This paper is organized as follows: in the next section, a brief discussion of the vehicle models for this study is presented. The overall ITB control system structure and control system development will be provided in section 3. Control actuation constraints will be discussed in section 4. Simulation results are shown in section 5 to prove the validity and the effectiveness of the proposed ITB vehicle dynamic control technology. Finally, the contributions and conclusions of the work are summarized in section 6.

II. Vehicle Model Development

In this study, two types of vehicle dynamic models have been developed for vehicle dynamic handling assistant analysis and control design purposes. The first one is a linear vehicle model that will be utilized for steady state analysis and control algorithm design. The second vehicle model is a nonlinear model for control system evaluation through comprehensive computer simulations. Both models represent a typical static understeer passenger vehicle.

The 2 DOF linear bicycle model, which is a good representation of the lateral vehicle dynamics in the linear handling region, is employed for steady state vehicle handling property analysis and active yaw dynamic controller design. It only includes the lateral vehicle dynamics of yaw rate r and side slip angle β. The linear vehicle dynamics can be described by the following state space equations based on small angle and constant longitudinal vehicle speed assumptions:

$$\begin{aligned} \dot{x} &= Ax + B\delta + B_c M_c \\ x &= (\beta, r)^T \\ A &= \begin{bmatrix} -\frac{C_{\alpha f}+C_{\alpha r}}{mU} & \frac{l_r C_{\alpha r}-l_f C_{\alpha f}}{mU^2} - 1 \\ \frac{l_r C_{\alpha r}-l_f C_{\alpha f}}{I_{zz}} & -\frac{l_f^2 C_{\alpha f}+l_r^2 C_{\alpha r}}{I_{zz}U} \end{bmatrix} \\ B &= \begin{bmatrix} \frac{C_{\alpha f}}{mU} \\ \frac{l_f C_{\alpha f}}{I_{zz}} \end{bmatrix}, \quad B_c = \begin{bmatrix} 0 \\ 1/I_{zz} \end{bmatrix} \end{aligned} \tag{4}$$

where m is the vehicle mass and I_{zz} is the yaw moment of inertia. l_f and l_r are illustrated in Figure 1. In the linear vehicle model, the vehicle longitudinal speed U is constant. The parameters C_{af} and C_{ar} are defined as the general axle cornering stiffness for the front axle and the rear axle respectively. The cornering stiffness is the gradient of lateral tire force versus tire slip angle following the SAE definition [10]. M_c is the active yaw control moment to be designed in this study for the purposes of handling assistant control and vehicle lateral stability improvement.

A non-linear vehicle handling model for simulation purposes has also been developed for this study. The 8 DOF

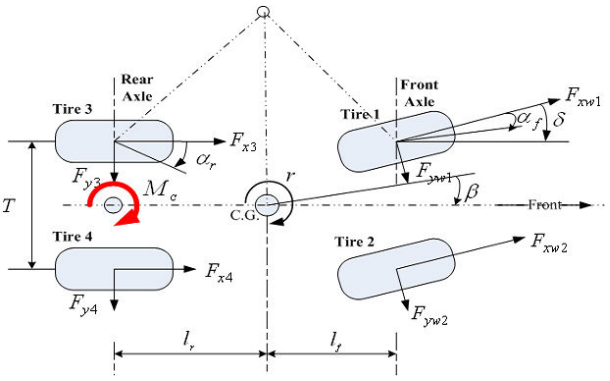

Fig. 1. The Vehicle Model and ITB Control Mechanism

nonlinear vehicle simulation model consists of the three planar motions plus sprung mass roll motion relative to the chassis and the rotational dynamics of the four wheels. The steering system is assumed to be stiff and only front wheel steering will be considered in this paper. The equations of motion for the nonlinear vehicle model are given as:

$$m(\dot{V}_x - V_y r) - m_s h \dot{r}\phi = \Sigma F_x \tag{5}$$
$$m(\dot{V}_y + V_x r) + m_s h \dot{r}\phi = \Sigma F_y \tag{6}$$
$$I_{zz}\dot{r} - I_{xz}\ddot{\phi} = \Sigma M_z \tag{7}$$
$$I_{xx}\ddot{\phi} + m_s h(\dot{V}_y + V_x r) - I_{xz}\dot{r} = \Sigma M_x \tag{8}$$
$$I_w \dot{\omega}_i = -R_w F_{xwi} + T_i \quad (i = 1, \cdots, 4) \tag{9}$$

$$\begin{aligned} \Sigma F_x &= F_{x1} + F_{x2} + F_{x3} + F_{x4} - F_l \\ \Sigma F_y &= F_{y1} + F_{y2} + F_{y3} + F_{y4} \\ \Sigma M_z &= l_f(F_{y1} + F_{y2}) - l_r(F_{y3} + F_{y4}) + M_c + M_d \\ \Sigma M_x &= [m_s g h - (K_{\phi f} + K_{\phi r})\phi - (D_{\phi f} + D\phi r)\dot{\phi} \\ m &= m_s + m_{uf} + mur \\ F_{yf} &= F_{y1} + F_{y2} \\ F_{yr} &= F_{y3} + F_{y4} \end{aligned}$$

where F_l is the simplified total vehicle resistance load. m_s and m_u are vehicle sprung mass and unsprung mass. I_{xx} is the roll moment of inertia. h_{cg} is the height of center of gravity. In the nonlinear vehicle dynamic model, the vehicle longitudinal speed is represented by V_x to differentiate with the constant speed U used in the linear vehicle model. The active yaw control moment generated by the ITB control system is generated from the rear axle tire longitudinal differential forces as in equation (1) and (2). Another key element in comprehensive vehicle simulations is the tire model, which incorporates physical nonlinearities to the simulation horizon. The STIREMOD tire model used in this study is capable of comprehensive tire force simulation covering the full operating range of the tire. For full details of STIREMOD see [11] for reference.

III. Control System Structure and Development

The first task in the ITB control system development is to understand the generic vehicle behavior in different driving

situations and to identify suitable control regions for different control objectives. To this end, the nonlinear vehicle dynamic property will be demonstrated in the vehicle side slip angle phase plane using a simplified 2 DOF yaw plane model. The phase plane of the vehicle side slip angle and the angular velocity are obtained using a two dimensional vehicle handling model under various initial conditions. The 2-D vehicle model is a simplified version of the nonlinear model in which only the lateral dynamics are being considered at constant vehicle speed setpoint:

$$mU\dot{\beta} = F_{yf} + F_{yr} - mUr \quad (10)$$

$$I_{zz}\dot{r} = l_f F_{yf} - l_r F_{yr} \quad (11)$$

where F_{yf} and F_{yr} are the lumped front and rear lateral tire forces computed from the nonlinear tire model.

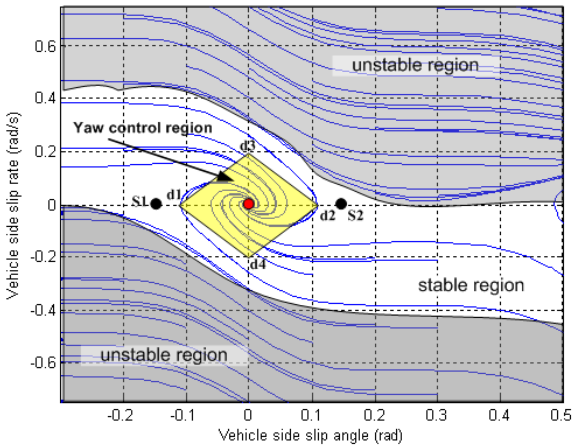

Fig. 2. Control Region Analysis at 75 kph

In Figure 2, vehicle trajectories at 75 kph are plotted on a $\beta - \dot{\beta}$ phase plane irrespective to steering input. Within a certain region, the vehicle trajectories will converge to the origin. On the other hand, vehicle trajectories outside that region will diverge, which indicates the loss of stability. The physical vehicle stability limit can be determined from the phase plane analysis illustrated. On the phase plane property, two saddle point (s_1, s_2) and one convergence point at the origin are identified. The yaw control region is determined as a diamond shaped area by the points (d_1, d_2) and intersections of $\dot{\beta}$ axis at (d_3, d_4). Within the yaw control region, the lateral vehicle dynamic has a strong stability conservation such that the vehicle is suitable for steering assistant control (yaw rate control) without violating the stability requirement. The study results also indicate that basic vehicle handling stability will become worse as vehicle speed increases or as friction condition gets lower. As a result, the stable region will shrink towards the origin. Outside this yaw control region, the vehicle is either marginally stable or it spins out as the vehicle side slip angle diverges. In this region, the ITB stability control is necessary to bring the vehicle dynamic back to a stable state.

The second task is to design an active yaw assistant and safety control algorithm using LQG control strategy. Basic designs are carried out at typical vehicle state setpoints based on the linear vehicle model. The design of an active yaw control system is an optimal disturbance rejection problem if the unforeseeable steering input is viewed as disturbance, i.e. an arbitrary signal in the bandwidth of the driver steering input. It is desirable to optimize the active yaw control system across the range of all possible steering inputs rather than in response to a constant steering value. The steering input can be modeled as colored noise by filtering white noise through a band limited low pass filter. In this paper, the filter used in [12] will be used in the ITB control system design. The steering input spectrum can be modeled approximately as:

$$S_\delta(\omega) = \frac{m_1}{\omega^2 + m_2} \quad (12)$$

This corresponds to a white noise filtered through a first order system, which has a cut-off frequency at m_2 rad/s and a static sensitivity value m_1. In state space, it can be represented as:

$$\dot{x}_f = A_f x_f + B_f w \quad (13)$$

$$\delta = C_f x_f \quad (14)$$

LQG minimizes a chosen performance index according to the application requirements set by the user. By selecting the weighting matrices Q and R properly, a balance can be achieved among the design objectives and control effort. The active yaw control system design is thus a tradeoff between minimizing yaw tracking error, constraining body sideslip motion and limiting energy consumption of the ITB actuation components. In this study, the weighting matrices Q and R penalize the desired output $x = [\beta - \beta_d, r - r_d]$ and the control input $u = M_c$, respectively. The desired yaw rate is modified from the linear vehicle model yaw rate output to smoothly limit the vehicle yaw rate based on the tire/road condition as follows:

$$r_d = sign\left(G_\gamma \delta\right) \cdot \min\left(\left|G_\gamma \delta\right|, \left|\frac{\mu g}{U}\right|\right) \quad (15)$$

$$\beta_d = \frac{G_\beta}{G_\gamma} r_d \quad (16)$$

where vehicle speed setpoint U is a low-pass filtered signal from instantaneous vehicle speed. G_β and G_γ are system steady state transfer gain from δ to β and r respectively

$$G_\beta = \frac{l_r - \frac{m_r}{C_{\alpha r}} U^2}{L + K_u U^2} \quad G_\gamma = \frac{U}{L + K_u U^2}$$

The linear vehicle model for control design purpose with the ITB yaw control moment M_c is given in equation (4). Define new control variable:

$$X = \begin{bmatrix} x_\beta \\ x_r \end{bmatrix} = \begin{bmatrix} \beta - \beta_d \\ r - r_d \end{bmatrix} \quad (17)$$

and incorporate the filter dynamics into this model, a new extended model is obtained as follows:

$$E\dot{\bar{X}} = \bar{A}\bar{X} + \bar{B}M_c, \quad Y = \bar{C}\bar{X} \quad (18)$$

The LQG control objective is designed as:

$$J = \int_0^\infty \left(Y^T Q Y + M_c^2 R\right) dt \tag{19}$$

The LQG feedback control law is

$$M_c = -K_{lqr}\bar{X} = -K_{lqr}[\beta - \beta_d, r - r_d, \delta/C_f]^T \tag{20}$$

where

$$E = \begin{bmatrix} 1 & 0 & C_f G_\beta \\ 0 & 1 & C_f G_r \\ 0 & 0 & 1 \end{bmatrix} \quad \bar{X} = \begin{bmatrix} x_\beta \\ x_r \\ x_f \end{bmatrix}$$

$$\bar{A} = \begin{bmatrix} A & BC_f \\ 0 & A_f \end{bmatrix}, \quad \bar{B} = \begin{bmatrix} 0 \\ \frac{1}{I_{zz}} \\ 0 \end{bmatrix}$$

$$\bar{C} = \begin{bmatrix} 1 & 0 & 0 \\ 0 & 1 & 0 \end{bmatrix}, \quad Q = \begin{bmatrix} q_1 & 0 \\ 0 & q_2 \end{bmatrix}$$

q_1, q_2 and R are all positive constants. By properly adjusting the weighting matrices, an optimal LQG feedback controller $M_c = -K_{lqr}X$ is obtained with specific weighting on control objectives. For example, the steering assistant control (yaw control) can be designed using $q_2 \gg q_1$ by exerting high penalty on the yaw rate tracking error. On the other hand, vehicle stability control law is designed using $q_1 \gg q_2$ by punishing excessive β values. Calibrating R with respect to q_1 and q_2 will balance on how much control effort the ITB system is going to exert to achieve a certain control objective. This is an important calibration consideration in the presence of actuation saturations.

In order to coordinate different control strategies, a control region based arbitrator is necessary in order to determine appropriate control action in different driving situations. The yaw control region is defined by the following equation:

$$\left|\beta - \beta_{ref} \pm \dot{\beta}\right| \leq d(U, \mu) \tag{21}$$

where the positive parameter d is a function of vehicle speed setpoint U and road friction coefficient μ. The value of d will decrease as U goes high and as μ reduces. When the vehicle state is in this region, steering enhancement control will be used to assist the driver in a turning maneuver. Stability control must be applied when the vehicle state is outside the yaw control region. In order to avoid unnecessary control law switches, the control arbitrator will only set the effective control law back to steering enhancement control if the stability control has been activated when all the following conditions are satisfied:

$$\left|\beta - \beta_{ref} \pm \dot{\beta}\right| \leq d(U, \mu) - d_{hyst}(U, \mu) \tag{22}$$

and

$$T_{stable} \geq t_{set}(U, \mu) \tag{23}$$

where d_{hyst} is a hysteretic parameter that requires that the vehicle achieve a higher level of stability conservation and remain in the compressed stable region for at least t_{set} time duration before releasing the stability control.

IV. Control Actuation Limit Analysis

For the ITB handling assistant control designed for a typical electrical drivetrain, the main system constraints come from the subsystem capabilities and the available support from the environment. In order to enable independent rear axle torque biasing, the electrical drivetrain must be able to deliver enough traction or braking torque to the wheels such that the requested direct yaw control moment can be generated. The drivetrain torque capability is bounded by the motor torque limits, motor toque gradient limits and electrical power limits that are determined by the battery SOC and temperature. In this study, a 30 kW motor is assumed to be installed on each rear wheel. Each is assumed to have a 1.4 Nm/ms torque gradient limit. The maximum regenerative braking power is assumed to be 14 kW with 626 Nm maximal wheel torque supply.

Besides the system power and torque limitations on the ITB actuation, another important ITB restriction is the ground friction condition. The minimum of the obtainable road friction force and the available powertrain torque supply determines how much ITB direct yaw control moment can be generated. While the powertrain system limitations are deterministic, the environmental limitations are imperceptible and unforeseeable in real applications. It is important to be able to estimate the ground friction condition such that proper control feedback gain can be selected to optimize the control function. To this end, a slip controller is included in the ITB control loop. The slip control system has the following control tasks: a). to estimate and feedback the approximate friction condition; b). to regulate wheel slip with respect to an optimal slip setpoint; c). to restrain wheel slip from entering the unstable slip region. A typical traction control algorithm has been used for these purposes. A more comprehensive slip controller has also been developed for the ITB control system as reported in [13].

V. Simulation verification

In this paper, the ITB handling assistant system is evaluated through nonlinear vehicle model simulations. The test case selected is an increasing magnitude sinusoidal steering maneuver. The vehicle is initially running at 75 kph and a cruise controller is implemented to regulate the vehicle speed around 75 kph using available traction capability. The steering input profile is shown in Figure 3, in which the vehicle road wheel steering angle magnitude linearly increases from zero to 25 degree in 50 seconds. The frequency of the sinusoidal steering signal is 0.75 Hz, which is close to the vehicle lateral dynamic's natural frequency. This maneuver is highly critical in terms of vehicle stability and steerability verification. In the low to medium steering level (0 to 10 degrees), the vehicle will gradually lose steerability in comparison with a linear vehicle's response property as the steering angle increases. As the vehicle becomes more and more in understeer, it is harder and harder to negotiate a turn. On the other hand, the vehicle side slip angle will increase at large steering levels especially when the friction condition is low. In the following analysis, the vehicle without active ITB

control system is named as passive vehicle and the vehicle under ITB control is named as active vehicle.

The first simulation test is carried out on dry asphalt ground where friction coefficient $\mu = 0.85$ is used. On a high μ surface, the passive vehicle keeps a high level of lateral force reservation in most of the driving scenarios. The main concern in handling assistant is the yaw rate degradation. Figure 4 and Figure 5 show the simulation results from the passive vehicle simulation. In these plots, a reference signal is indicated by "ref" and FL, FR, RL and RR denote signals associated to the four wheels. Even though the passive vehicle remains stable, it cannot properly follow the driver's steering input. The passive vehicle starts showing yaw rate degradation after 7 seconds from where the nonlinear vehicle's yaw rate is less than the reference yaw rate as shown in the bottom plot of Figure 4. As a result, the passive vehicle's side slip angle is also less than the reference level as shown in the top plot of Figure 5.

In the next simulation, an active vehicle is used and the simulation results are plotted in Figure 6 and Figure 7. From the bottom plot of the Figure 6, it is clear that the vehicle steering performance has been largely improved as the nonlinear vehicle yaw rate tracks the reference yaw rate accurately. Additionally, the ITB controller releases the yaw rate tracking accuracy in the presence of large side slip angle in order to reserve vehicle stability. The tracking error becomes noticeable at the handling limit for the active vehicle. This is due to the functional limitation of the stand-alone steerability controller in bounding the sideslip motion of the vehicle at the handling limit. The steering enhancement control is active before around 22 seconds. Excessive side slip motion is identified at around 22 seconds by the control arbitrator and it switches the ITB to the stability control. After that, the stability controller restrains the side slip motion in the presence of a large steering input and the active vehicle's side slip angle is confined within ± 0.1 rad. This ensures that the vehicle lateral stability is guaranteed. Control region 1 indicates yaw control region and control region 3 indicates stability control region. Control Region 0 indicates no active ITB control.

The next simulation is low friction condition test where the vehicle stability is critical due to a low level of lateral force reservation. The friction coefficient used in this simulation is $\mu = 0.2$. The passive vehicle simulation results are given in Figure 8 and Figure 9. During this critical maneuver, the passive vehicle reaches the handling limit at around 30 seconds in this alternating sequence and the vehicle spins out as the side slip angle become quite large (more than 45^o). On the other hand, the active vehicle keeps stable vehicle motion and it follows the reference yaw rate in satisfactory accuracy as shown in Figure 10 and Figure 11. Throughout the test, the vehicle side slip angle is confined in ± 0.05 rad level. The vehicle stability control objective is achieved.

VI. Conclusion and Future Work

In this paper, a vehicle handling assistant control system has been developed to improve vehicle steerability and

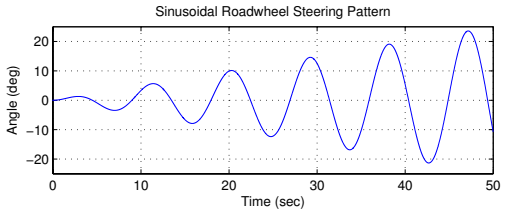

Fig. 3. Sinusoidal maneuver test steering profile

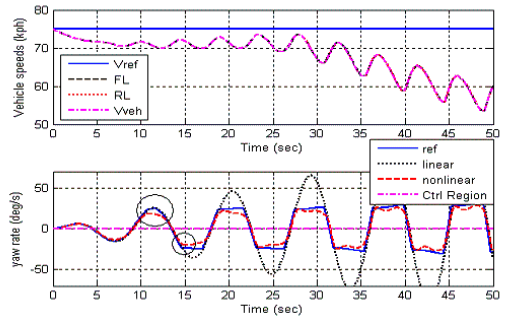

Fig. 4. Passive vehicle simulation on high μ ground part I

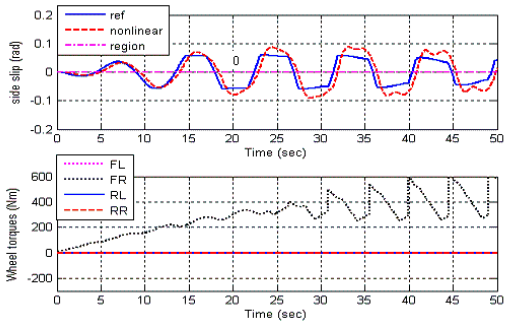

Fig. 5. Passive vehicle simulation on high μ ground part II

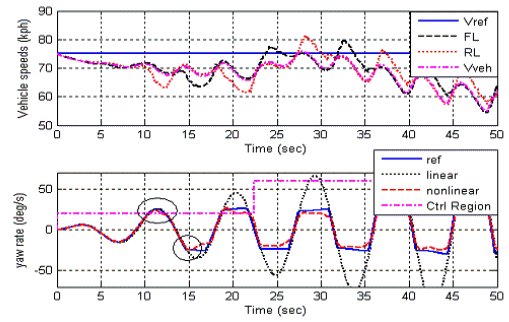

Fig. 6. Active vehicle simulation on high μ ground part I

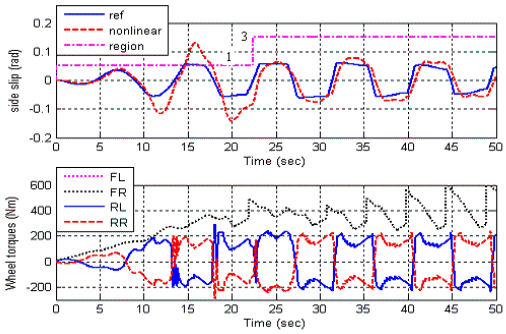

Fig. 7. Active vehicle simulation on high μ ground part II

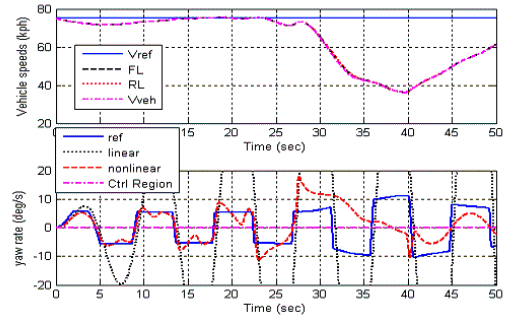

Fig. 8. Passive vehicle simulation on low μ surface part I

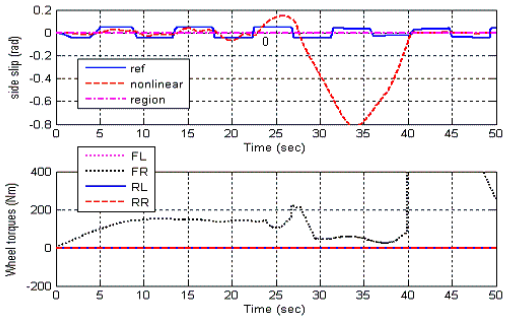

Fig. 9. Passive vehicle simulation on low μ surface part II

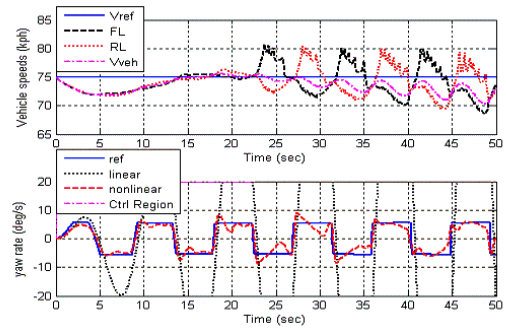

Fig. 10. Active vehicle simulation on low μ surface part I

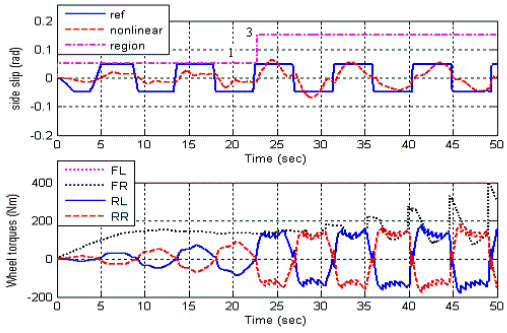

Fig. 11. Active vehicle simulation on low μ surface part II

stability in dynamic vehicle handling maneuvers utilizing the proposed ITB technology. A basis has been established for the application of ITB technology for the dynamic control of a hybrid electric vehicle. In future work, control actuation issues, control consistency and robustness will be addressed. The driver's responses to the ITB controlled vehicle will be evaluated in different control scenarios. Furthermore, extensions of the torque biasing technology to all driven wheels are being studied to further expand the application scenarios.

REFERENCES

[1] J. Ackermann, "Robust control prevents car skidding," *IEEE Control System Magazine*, vol. 17(3), pp. 23–31, 1997.

[2] E. Ono, S. Hosoe, S. Doi, K. Asano, and Y. Hayashi, "Theoretical approach for improving the vehicle robust stability and maneuverability by active front wheel steering control," *Vehicle System Dynamics*, vol. 28, pp. 748–753, 1998.

[3] S. Mammar and D. Koenig, "Vehicle handling improvement by active steering," *Vehicle System Dynamics*, vol. 38(3), pp. 221–242, 2002.

[4] S. Motoyama, H. Uki, K. Isoda, and H. Yuasa, "Effect of traction force distribution control on vehicle dynamics," *Vehicle System Dynamics*, vol. 22, pp. 455–464, 1993.

[5] S. Inagaki, I. Kshiro, and M. Yamamoto, "Analysis on vehicle stability in critical cornering usng phase-plane method," in *In Proceedings of the 2nd International Symposium on Advanced Vehicle Control (AVEC'94)*, Tsukuba, Japan, 1994, pp. 287–292.

[6] B. Post, X. Kang, and C. Cymbal, "Method for improved yaw stabilization control by ingetration of a direct yaw control awd system with a vehicle stability assist controller," *SAE Paper 2008-01-1456*, 2008.

[7] B. Post, X. Kang, and T. Klaus, "The influence of direct yaw control awd system on vehicle stability and response in all driving conditions," *SAE Paper 2008-01-0591*, 2008.

[8] L. Kakalis, A. Zorzutti, F. Cheli, and G. Travaglio, "Brake based torque vectoring for sport vehicle performance improvement," *SAE Paper 2007-01-0596*, 2008.

[9] F. Tahami, R. Kzaemi, and S. Farhanghi, "Direct yaw control of an all wheel drive ev based on fuzzy logic and neutral networks," *SAE Paper 2003-01-0956*, 2003.

[10] T. D. Gillespie, *Fundamentals of Vehicle Dyanmics*. Warrendale, Pennsylvania: SAE, 1992.

[11] R. Allen, R. Magdaleno, T. Rosenthal, D. Klyde, and J. Hogue, "Tire modeling requirements for vehicle modeling," *SAE Paper 950312*, 1995.

[12] H. Yu, L. Guvenc, and U. Ozguner, "Heavy duty vehicle rollover detection and active roll control," *Vehicle System Dynamics*, vol. 46:6, p. 451 470, 2008.

[13] W. Liang, H. Yu, R. McGee, M. Kuang, and J. Medanic, "Vehicle pure yaw moment generation by using modified-lugre dynamic tire model," in *To be appeared in the Preceedings of the 2009 American Control Conference*.